sonic aircraft. In addition to its use for determining flight profiles for minimum time to climb to a given altitude and speed, and minimum fuel to climb to a given altitude and speed, this paper shows that the energy-state approximation may also be used to determine flight profiles for 1) maximum-range glide from a given altitude and speed to another altitude and speed; 2) maximum range at a fixed throttle setting for a given amount of fuel (or, what is the equivalent problem, minimum fuel for a given range at a fixed throttle setting); 3) maximum total range for a given amount of fuel (or minimum fuel for a given total range); 4) maximum range in a given time (or minimum time for a given range).

References

[1] Perkins, C. D. and Hage, R. E., *Airplane Performance, Stability, and Control*, Wiley, New York, 1949, pp. 175–182.

[2] Lush, K. J., "A Review of the Problem of Choosing a Climb Technique with Proposals for a New Climb Technique for High Performance Aircraft," R and M 2557, 1951, British Aeronautical Research Council.

[3] Rutowski, E. S., "Energy Approach to the General Aircraft Performance Problem," *Journal of Aeronautical Science*, Vol. 21, No. 3, March 1954, pp. 187–195.

[4] Lush, K. J. et al., "Total Energy Methods," *AGARD Flight Test Manual*, Vol. 1, 1954, Chap. 7.

[5] Kelley, H. J., "An Investigation by Variational Methods of Flight Paths for Optimum Performance," Ph.D. thesis, New York Univ., May 1958.

[6] Miele, A., "Minimal Maneuvers of High Performance Aircraft in a Vertical Plane," TN D-155, Sept. 1959, NASA.

[7] Miele, A., *Flight Mechanics I—Theory of Flight Paths*, Addison-Wesley, Reading, Mass., 1962.

[8] Bryson, A. E. and Denham, W. F., "A Steepest-Ascent Method for Solving Optimum Programming Problems," *Journal of Applied Mechanics*, Vol. 29, June 1962.

[9] Denham, W. F., "Steepest-Ascent Solution of Optimal Programming Problems," Ph.D. dissertation, Div. of Engineering and Applied Physics, Harvard Univ., 1963, Chap. 6.

NOV.-DEC. 1969 J. AIRCRAFT VOL. 6, NO. 6

Lifting-Surface Theory for V/STOL Aircraft in Transition and Cruise. I

E. S. LEVINSKY*, H. U. THOMMEN†, P. M. YAGER‡, AND C. H. HOLLAND‡
Air Vehicle Corporation, San Diego, Calif.

This is the first part of a two-part paper in which a large-tilt-angle lifting-surface theory is developed for tilt-wing and tilt-propeller (or rotor) type V/STOL aircraft. Part I deals with the development of an inclined actuator disk analysis which forms the basis of the method. Closed form solutions are obtained for the velocity potential at large distances behind the actuator surface. Both the normal velocity and the nonlinear pressure boundary conditions are satisfied across the slipstream interface. Effects of slipstream rotation are also evaluated. In Part II, the included actuator disk analysis is combined with a discrete-vortex Weissinger-type lifting-surface theory for application to wing-propeller combinations at arbitrary tilt angle and forward speed.

Nomenclature

A_p = propeller area
A_s = area of fully contracted propeller slipstream
b = wing span
C_{D_0} = zero lift drag coefficient
C''_{H_p} = propeller horizontal force coefficient based on propeller area and slipstream total pressure
C''_{L_p} = propeller vertical force coefficient based on propeller area and slipstream total pressure
C_l = section lift coefficient based on q_∞
C_{l_a} = section ideal lift coefficient
C, D = unknown coefficients in Eqs. (4) and (5)
C''_n = section normal force coefficient based on slipstream total pressure
c = wing chord length
$\mathbf{D}$ = drag force
$\mathbf{e}_r, \mathbf{e}_x, \mathbf{e}_\theta$ = unit vectors in cylindrical coordinate system
$\mathbf{e}_z$ = unit vector in z direction
F = complex potential (inclined actuator disk theory)
G = integral defined by Eq. (24)
$g(\mu)$ = function of $\mu = (1 + \mu)(1 - \mu)^{-1}G_o$
H = total pressure
h = one-half of the vortex spacing on the wing
I = integral defined by Eq. (24), also number of wing control stations
i = $(-1)^{1/2}$
J = propeller advance ratio
K = number of slipstreams
L = lift force
M = number of slipstream control points
N = propeller revolutions/sec
n = normal force/unit span
P, P' = power, also potential influence function (P' for multiple slipstreams)
p = static pressure
q = dynamic pressure
R = radius of fully contracted slipstream
R_c = radius of cylindrical control surface
R_p = propeller radius
r, θ = cylindrical coordinates, slipstream coordinate system
S = surface area, also downwash velocity influence coefficient
T = propeller thrust
T''_c = propeller thrust coefficient = $T/A_p(q_\infty + \Delta H)$
u, v, w = velocity components in slipstream coordinate system
V = velocity
V_γ = induced velocity inside slipstream

Received September 26, 1968; revision received April 23, 1969. The research was supported by the U. S. Army Aviation Material Laboratories under Contract No. DAAJ02-67-C-0059, and has been reported in more detail in Ref. 15.

* Vice President. Member AIAA.

† Former Staff Scientist, now Professor at Southeastern Massachusetts Technical Institute, Department of Mechanical Engineering, North Dartmouth, Mass.

‡ Staff Scientists.

V_∞ = freestream velocity
V_R = resultant velocity
v_θ = swirl velocity
w_∞ = component of freestream velocity in z direction
X = component of propeller force in x direction
x, y, z = slipstream coordinate system
x', y', z' = freestream coordinate system
y_p = spanwise position of propeller centerline
Z = component of propeller force in z direction, also complex variable $Z = re^{i\theta} = y + iz$
α = wing angle of attack
α_a = ideal angle of attack
α_{eff} = effective angle of attack
α_p = propeller tilt angle
α_δ = flap effectiveness parameter
Γ = vortex strength
γ = ring vortex strength/unit length
Δ = difference operator
$\Delta\theta_n$ = vortex spacing on slipstream(s)
δ = inclination of slipstream vortex tube with respect to the freestream
δ_f = flap angle
δ_{mn} = Kronecker delta
ϵ = downwash angle
ζ = unknown function of θ
θ = polar coordinate (r, θ) in slipstream coordinate system
μ = ratio u_0/u_s
ν_t = effective turbulent kinematic viscosity
ρ = density
φ = velocity perturbation potential
φ' = reduced velocity perturbation potential $= \mu\varphi$
$\varphi_{s\Gamma}, \varphi_{o\Gamma}$ = perturbation potentials due to wing and slipstream horseshoe vortex systems
ψ = stream function
Ω = effective origin of propeller viscous core ahead of $c/4$ point
∇ = gradient operator

Subscripts

a = ideal
i, j = summation indices over wing
k, l = summation indices over the number of slipstreams
m, n = summation indices over the slipstream(s)
o = outside slipstream
p = propeller
R = resultant
s = inside slipstream
u = upper boundary of slipstream
Γ = induced by wing and slipstream vortex elements
γ = induced by ring vortices
∞ = freestream

Superscripts

$-$ = normalized quantity defined by Eq. (24)
$*$ = complex conjugate

I. Introduction

CONSIDERABLE research effort has been expended in the past pertaining to the interaction between a wing and slip stream. Most noteworthy is the pioneering contribution of Koning,[1] who formulated the proper boundary conditions across the interface of an uninclined slipstream. Koning matched both pressure and flow angle on each side of the boundary within the limitations of linearized theory and used the Prandtl lifting line theory to predict slipstream interference effects at cruise speeds. Koning's treatment was extended to a wider range of forward speeds by Glauert[2] and by Franke and Weinig.[3] The latter authors also improved and generalized the theory to include effects of small propeller inclination and slipstream rotation. Nevertheless, comparison with test data indicated that the theory overpredicted the additional wing lift inside the slipstream by a substantial margin.[4]

Partly because of this failure of the lifting line approach, which was assumed due to the low aspect ratio of the wing segment inside the slipstream, Graham et al.[5] supplemented the lifting-line theory with lifting-surface (Weissinger) and slender body theories, and found improved agreement with test data. The Weissinger lifting-surface theory was subsequently generalized in a series of papers by Ribner and Ellis[6–8] to apply to multiple uninclined slipstreams of arbitrary cross section. The latter authors introduced horseshoe vortex elements of unknown strength along the wing $\frac{1}{4}$-chord line, and required that the wing boundary condition be satisfied at the $\frac{3}{4}$-chord line in accordance with the standard Weissinger approach. By considering a reduced velocity potential inside the slipstream, they were able to satisy both the pressure and flow angle boundary conditions across the slipstream(s) through introduction of an additional set of unknown horseshoe vortex elements around the slipstream periphery. Calculations carried out for a wing and a single uninclined slipstream showed good agreement with the test data of Brenckmann.[9]

It is clear that the theory of wing-propeller interaction must be extended to include effects of large slipstream inclination if the theory is to be applicable for tilt-wing or tilt-rotor type V/STOL aircraft. Previous attempts to treat inclined slipstreams have been unsuccessful, partly because of the use of a solid cylinder approximation for the inclined slipstream, e.g., Refs. 5 and 8. Although the solid cylinder produces a disturbed flowfield outside the slipstream which satisfies the normal velocity boundary condition, the nonlinear pressure boundary condition is not satisfied. The rectification of this inadequacy and the development of a wing-slipstream interaction theory applicable to V/STOL technology are the motivation for the present study.

In Part I of the present paper, a new inclined actuator disk theory, which satisfies both the normal velocity and nonlinear pressure boundary conditions across the slipstream interface, is derived. Effects of slipstream rotation are included by adopting a viscous core vortex model inside the slipstream for the swirl velocities. The major assumptions in the resulting analysis are that the slipstream is fully contracted, of basically circular cross section, and of constant total head (but with nonuniform velocities and static pressures) in the region of the wing.

The inclined actuator disk theory is combined in Part II with the Ribner-Ellis lifting surface method to treat tilt-rotor or propeller-wing combinations at large tilt angles and at forward speeds from hover to cruise. The resulting generalized theory is compared wherever possible with available experimental data. In addition, an extensive series of calculations is carried out to provide theoretical data for span loading, downwash angles, and dynamic pressure in the wake and slipstream for representative two- and four-slipstream V/STOL configurations and flight conditions.

II. Inclined Actuator Disk Theory

Boundary Conditions and General Solution

The incompressible flowfield created by an actuator disk with its axis inclined to the freestream direction at an angle α_p is to be considered (Fig. 1). The air passing through the actuator disk is assumed to experience a uniform increase in total and static pressure of magnitude ΔH, so that the total pressure inside the slipstream has the constant value $H_s = H_0 + \Delta H$, where H_0 is the total pressure outside the slipstream. The resultant force on the actuator disc is assumed to act normal to the disk surface, and is of magnitude $A_p\Delta H$. In this respect, the actuator disk differs from an inclined propeller or rotor which develops forces in the plane of rotation. This in-plane force is usually small compared to the normal force, and is neglected in the present formulation.

We next assume that this flowfield can be approximated far behind the actuator disk by a distribution of suitable singularities around the surface of a semi-infinite circular tube (Fig. 1). The axis of the tube is inclined to the freestream by

the angle δ. This is the angle at which the slipstream would be inclined far behind the disk if not for distortion. The radius of the tube is taken as that of the fully contracted slipstream $r = R$, and the boundary conditions which must hold across a fluid interface are satisfied on the surface of the tube.

A slipstream coordinate system x, y, z (or equivalently x, r, θ) with the x axis coincident with the tube axis is introduced for convenience. Denoting by $\mathbf{V}_o$, $\mathbf{V}_s$ the velocities outside and inside the slipstream, respectively, the boundary condition on the velocity components normal to the slipstream boundary is

$$\mathbf{e}_r \cdot \mathbf{V}_o / \mathbf{e}_x \cdot \mathbf{V}_o = \mathbf{e}_r \cdot \mathbf{V}_s / \mathbf{e}_x \cdot \mathbf{V}_s \qquad \text{for } r = R \tag{1}$$

where $\mathbf{e}_x$, $\mathbf{e}_r$, $\mathbf{e}_\theta$ are unit vectors in the designated directions (Fig. 1). Equation (1) signifies that the flow angles normal to the cylindrical surface are the same across the interface, but allows a discontinuity in the velocity components in the plane of the surface.

The axial velocity components of $\mathbf{V}_o$ and $\mathbf{V}_s$ are designated by $\mathbf{e}_x u_o$ and $\mathbf{e}_x u_s$, respectively, and may be regarded as constant at large distances from the actuator disk. However, the cross-flow velocity components are nonuniform, even for large x, and lead to deformation of the originally circular slipstream.

A second boundary condition is that the static pressures $p_o(r, \theta)$ and $p_s(r, \theta)$ outside and inside the slipstream, respectively, are identical on the tube surface. It will prove convenient in the analysis to change the flow into one of constant total head by subtracting ΔH from the pressure p_s inside the slipstream. The pressure boundary condition is then

$$p_o(R, \theta) - p_s(R, \theta) = \Delta H \tag{2}$$

The above flowfield may be obtained by suitably distributing singularities on the surface of the cylindrical tube. First, consider a distribution of ring vortices $\boldsymbol{\gamma} = \mathbf{e}_\theta[d\Gamma(x)/dx]$ with axes coincident with the x axis and with strength Γ. Restricting ourselves to large distances behind the actuator disk, the ring vortex distribution may be regarded as infinitely long and of uniform strength. It will therefore induce only axial velocity components inside the tube, and will have no influence outside the tube. The derivative γ is chosen so that the induced velocity $\mathbf{V}_\gamma$ inside the tube is $\mathbf{e}_x(u_s - u_o)$, viz.,

$$\lim_{x \to \infty} \mathbf{V}_\gamma = \mathbf{e}_x \gamma = \mathbf{e}_x(u_s - u_o), \quad r < R$$
$$\lim_{x \to \infty} \mathbf{V}_\gamma = 0, \quad r > R \tag{3}$$

Next, a distribution of vortices and sources and sinks with axes parallel to x is introduced. These singularities will vary in strength as a function of θ, but can be assumed independent of x when $x \to \infty$. In this limit, and using symmetry conditions about $\theta = \pm \pi/2$, the most general form of the resulting two-dimensional velocity perturbation potential may be written as

$$\varphi = \varphi_s = -\sum_{n=1,3,5}^{\infty} \frac{RC_n(r/R)^n}{n} \sin n\theta, \quad r < R \tag{4}$$

$$\varphi = \varphi_o = \sum_{n=1,3,5}^{\infty} \frac{RD_n(r/R)^{-n}}{n} \sin n\theta, \quad r > R \tag{5}$$

Thus, the resultant velocities become for $x \to \infty$

$$\mathbf{V}_s = \mathbf{V}_\infty + \mathbf{e}_x(u_s - u_o) + \nabla\varphi_s = \mathbf{e}_x u_s + \mathbf{e}_z w_\infty + \nabla\varphi_s, \quad r < R \tag{6}$$

$$\mathbf{V}_o = \mathbf{V}_\infty + \nabla\varphi_o = \mathbf{e}_x u_o + \mathbf{e}_z w_\infty + \nabla\varphi_o, \quad r > R \tag{7}$$

where the undisturbed freestream velocity $\mathbf{V}_\infty$ has been resolved into components

$$\mathbf{V}_\infty = \mathbf{e}_x u_o + \mathbf{e}_z w_\infty$$

with $u_o = V_\infty \cos\delta$ and $w_\infty = V_\infty \sin\delta$.

Evaluation of the Unknown Coefficients

The coefficients C_n, D_n, which must be known to obtain the velocity field, are determined from the boundary conditions on the slipstream interface.

Making use of Eqs. (6) and (7), the normal velocity condition [Eq. (1)] becomes

$$(\partial\varphi_o/\partial r) - \mu(\partial\varphi_s/\partial r) = -(1 - \mu)w_\infty \sin\theta, \quad r = R \tag{8}$$

where $\mu = u_o/u_s$.

Introducing Eqs. (4) and (5), and satisfying Eq. (8) for each term in $\sin n\theta$, gives the following conditions on the coefficients:

$$D_1 - \mu C_1 = (1 - \mu)w_\infty$$
$$D_n = \mu C_n, \qquad n \geq 3 \tag{9}$$

Utilizing the steady form of the incompressible Bernoulli equation, the pressure condition [Eq. (2)] may be similarly expressed as

$$2\,\Delta H/\rho = u_s^2 - u_o^2 + [\mathbf{e}_z w_\infty + \nabla\varphi_s]^2 - [\mathbf{e}_z w_\infty + \nabla\varphi_o]^2, \qquad r = R \tag{10}$$

where the density ρ is taken the same inside and outside the slipstream. Since $\nabla\varphi_s$ and $\nabla\varphi_o$ are both functions of θ, whereas the remaining quantities in Eq. (10) are independent of θ, it is required that

$$2\Delta H/\rho = u_s^2 - u_o^2, \qquad r = R$$

or, equivalently,

$$\Delta H/q_\infty = [(1 - \mu^2)/\mu^2] \cos^2\delta, \qquad r = R \tag{11}$$

in order that Eq. (10) be satisfied. The pressure condition thereupon becomes, using complex notation

$$|iw_\infty + \Delta\varphi_s| = |iw_\infty + \Delta\varphi_o|, \qquad r = R$$

which may be written, without loss of generality, as

$$e^{i\zeta(\theta)}(w_\infty - i\nabla\varphi_s) = w_\infty - i\nabla\varphi_o, \quad r = R \tag{12}$$

where ζ is an unknown function of θ to be determined, and $\nabla\varphi = (\partial\varphi/\partial y) + i(\partial\varphi/\partial z)$. Substituting Eqs. (4), (5), and (9) into Eq. (12) for $r = R$, and observing that all coefficients C_n, D_n are real, it is readily determined that ζ must be either 0 or π. Taking first $\zeta = 0$,§ and equating coefficients of like powers of $e^{i\theta}$ on both sides of Eq. (12) gives

$$C_1 = 0$$
$$C_3 = -(1 - \mu)w_\infty \tag{13}$$
$$C_{n+2} = -\mu C_n \quad n \geq 3$$

Complex perturbation potential

In terms of the complex potentials $F_s = \varphi_s + i\psi_s$ and $F_o = \varphi_o + i\psi_o$ inside and outside the slipstream, respectively, Eqs. (4) and (5) yield

$$\frac{dF_s}{dZ} = i \sum_{n=1,3,\ldots} C_n \left(\frac{Z}{R}\right)^{n-1}$$
$$\frac{dF_o}{dZ} = -i \sum_{n=1,3,\ldots} \frac{D_n}{(Z/R)^{n+1}} \tag{14}$$

§ The rejection of solutions with $\zeta = \pi$ is justified in the next section.

where

$$\frac{dF}{dZ} = \left(\frac{\partial\varphi}{\partial r}\cos\theta - \frac{1}{r}\frac{\partial\varphi}{\partial\theta}\sin\theta\right) - i\left(\frac{\partial\varphi}{\partial r}\sin\theta + \frac{1}{r}\frac{\partial\varphi}{\partial\theta}\cos\theta\right)$$

and $Z = re^{i\theta}$.

By inserting Eqs. (9) and (13) for the coefficients C_n, D_n in Eqs. (14), it is found that the series can be readily summed. The resulting closed form expressions may be integrated with respect to Z, giving

$$F_s = -i\frac{(1-\mu)}{\mu}w_\infty Z + \frac{(1-\mu)}{2\mu^{3/2}}w_\infty R\ln\left[\frac{Z/R - i/\mu^{1/2}}{Z/R + i/\mu^{1/2}}\right] \quad (15)$$

$$F_o = -\frac{(1-\mu)}{2\mu^{1/2}}w_\infty R\ln\left[\frac{Z/R - i\mu^{1/2}}{Z/R + i\mu^{1/2}}\right] \quad (16)$$

In the limit $\mu \to 1$, which corresponds to an actuator disk of vanishing strength, $\Delta H \to 0$ and F_s and F_o vanish, indicating that the flowfield is undisturbed in this limit. Re-evaluation of the coefficients for $\zeta = \pi$ yields expressions similar in form to Eqs. (15) and (16), except that the factor $(1 - \mu)$ is replaced by $(1 + \mu)$. These solutions must be discarded, because they fail to satisfy the physical flow in the limit $\mu \to 1$.

In the limit $\mu \to 0$, corresponding either to an inclined actuator disk of infinite strength ($\Delta H \to \infty$) or at zero forward velocity, expansion of the logarithmic term in Eq. (16) shows that F_o becomes the complex potential produced by a doublet at the origin. Upon superposition of the component w_∞ of the freestream velocity parallel to the z axis, the resultant outside flow velocity becomes the same as if the slipstream boundary were a solid surface. The solid cylinder approximation for an inclined slipstream, which was discussed in the Introduction, is found to hold only in this limit.

At intermediate values of μ, the complex perturbation potential F_o is recognized as that due to a source of strength $\pi(1 - \mu)w_\infty R/\mu^{1/2}$ located at $Z = -iR\mu^{1/2}$ and to a sink of equal strength located at $Z = iR\mu^{1/2}$. Similarly, F_s is that of a source and sink at $Z = \pm iR/\mu^{1/2}$, together with a parallel flow of velocity $(1 - \mu)w_\infty/\mu$ in the positive Z direction.

Velocity field

Having obtained the complex potential in the Trefftz plane $x = \infty$, the over-all velocity field is readily evaluated from

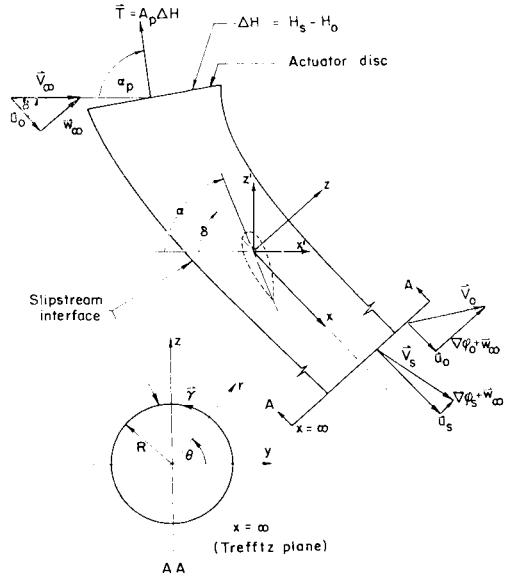

Fig. 1 Flow model and coordinate systems, inclined actuator disk theory.

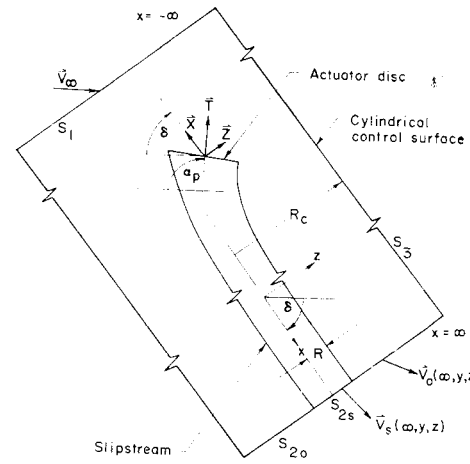

Fig. 2 Control surface for determination of forces and power, inclined actuator disk theory.

Eqs. (6) and (7). The velocity potentials φ_s and φ_o are found by extracting the real parts of F_s and F_o, respectively. Thus, in rectangular coordinates,

$$\varphi_s = \frac{(1-\mu)}{\mu}w_\infty z - \frac{(1-\mu)}{4\mu^{3/2}}w_\infty R \times \ln\left[\frac{y^2 + z^2 + R^2/\mu + 2Rz/\mu^{1/2}}{y^2 + z^2 + R^2/\mu - 2Rz/\mu^{1/2}}\right] \quad (17)$$

$$\varphi_o = \frac{(1-\mu)}{4\mu^{1/2}}w_\infty R\ln\left[\frac{y^2 + z^2 + R^2\mu + 2Rz\mu^{1/2}}{y^2 + z^2 + R^2\mu - 2Rz\mu^{1/2}}\right] \quad (18)$$

Taking the gradient of the above expressions and substituting into Eqs. (6) and (7), the over-all velocity components u, v, w in the x, y, z directions at any arbitrary point in the flowfield are found to be

$$u_o = V_\infty\cos\delta$$

$$v_o = -\left\{\frac{2(1-\mu)yz}{[y^2 + (z - R\mu^{1/2})^2][y^2 + (z + R\mu^{1/2})^2]}\right\} \times R^2V_\infty\sin\delta \quad (19)$$

$$w_o = \left\{1 + \frac{(1-\mu)R^2(y^2 - z^2 + \mu R^2)}{[y^2 + (z - R\mu^{1/2})^2][y^2 + (z + R\mu^{1/2})^2]}\right\} \times V_\infty\sin\delta$$

for $y^2 + z^2 > R^2$, and

$$u_s = V_\infty\cos\delta/\mu$$

$$v_s = \left\{\frac{z(1-\mu)yz}{[\mu y^2 + (\mu^{1/2}z - R)^2][\mu y^2 + (\mu^{1/2}z + R)^2]}\right\} \times R^2V_\infty\sin\delta \quad (20)$$

$$w_s = \left\{1 - \frac{(1-\mu)R^2(\mu y^2 - \mu z^2 + R^2)}{[\mu y^2 + (\mu^{1/2}z - R)^2][\mu y^2 + (\mu^{1/2}z + R)^2]}\right\} \times V_\infty\frac{\sin\delta}{\mu}$$

for $y^2 + z^2 < R^2$.

Equations (19) and (20) give the velocities in the flowfield at $x = \infty$ in terms of the parameters μ and δ. Before applying these expressions to evaluating the downwash angle distribution inside as well as outside the slipstream, it will prove convenient to express μ and δ in terms of parameters of more physical significance. This will be accomplished in the next section by relating μ and δ to the tilt angle α_p and thrust coefficient T''_c. It will also be convenient to relate the vortex tube radius R to the physical radius of the disk R_p.

Forces and Power on an Inclined Actuator Disk

Continuity of mass and momentum flux

In order to evaluate the forces acting on the disk, a cylindrical control tube of radius R_c is placed around the disk and slipstream as shown in Fig. 2. The value of R_c is taken sufficiently large so that the pressure is ambient around the cylindrical surface S_3. The velocity is assumed to be equal to $\mathbf{V}_\infty$ on the forward face S_1 at $x = -\infty$, and to be given by Eqs. (19) and (20) on the rear face S_2 at $x = \infty$. The continuity equation is written in integral form as

$$\int_{S_1} \mathbf{V}(-\infty)\cdot d\mathbf{S} + \int_{S_{2s}+S_{2o}} \mathbf{V}(\infty)\cdot d\mathbf{S} + \int_{S_3} \mathbf{V}(R_c)\cdot d\mathbf{S} = 0$$

where $d\mathbf{S}$ has the direction of the inward normal to the surface, and the subscripts s and o designate the portions of S_2 inside and outside the slipstream, respectively. Using Eqs. (6) and (7), the net mass flux into the cylindrical surface becomes, for a unit density,

$$\int_{S_3} \mathbf{V}(R_c)\cdot d\mathbf{S} = \pi R^2(u_s - u_o)$$

and carries a net momentum flux

$$\int_{S_3} \mathbf{V}(\mathbf{V}\cdot d\mathbf{S}) = \pi R^2(u_s - u_o)\mathbf{V}_\infty \tag{21}$$

The momentum equation is expressed in the form

$$\mathbf{T} = -\rho \int_{S_1+S_2+S_3} \mathbf{V}(\mathbf{V}\cdot d\mathbf{S}) - \int_{S_1+S_2+S_3} p\, d\mathbf{S} \tag{22}$$

where $\mathbf{T}$ is the thrust force normal to the actuator disk. Taking the component of $\mathbf{T}$ in the x direction and making use of Eqs. (6), (7), (11), and (21), together with the incompressible form of Bernoulli's equation, we obtain after some rearrangement

$$X = \pi R^2 \rho u_s(u_s - u_o) - \frac{1-\mu^2}{2\mu^2}\rho w_\infty{}^2 \pi R^2 - \rho w_\infty{}^2 \left[I_o + \frac{I_s}{\mu^2} + \frac{1}{2}\left(G_o + \frac{G_s}{\mu^2} \right) \right] \pi R^2 \tag{23}$$

Here, we have defined

$$I_o = \frac{1}{\pi R^2}\int_{S_{2o}} \frac{\partial \bar{\varphi}_o}{\partial z}\, dS \qquad I_s = \frac{1}{\pi R^2}\int_{S_{2s}} \frac{\partial \bar{\varphi}_o}{\partial z}\, dS$$

$$G_o = \frac{1}{\pi R^2}\int_{S_{2o}} (\nabla \bar{\varphi}_o)^2 dS \qquad G_s = \frac{1}{\pi R^2}\int_{S_{2s}} (\nabla \bar{\varphi}_s)^2 dS \tag{24}$$

where $\bar{\varphi}$ is a modified velocity potential such that

$$\partial\bar{\varphi}_o/\partial z = (1/w_\infty)(\partial\varphi_o/\partial z)$$

$$\partial\bar{\varphi}_o/\partial y = (1/w_\infty)(\partial\varphi_o/\partial y)$$

$$\partial\bar{\varphi}_s/\partial z = (\mu/w_\infty)(\partial_s/\partial z) - (1-\mu)$$

$$\partial\bar{\varphi}_s/\partial y = (\mu/w_\infty)(\partial_s/\partial y)$$

Evaluation of integrals

The integrals given by Eq. (24) will be evaluated below. Initially, we consider I_o. Integrating first with respect to z, and recognizing that $\lim_{z\to\pm\infty} \bar{\varphi}_o = 0$, we obtain from the first of Eqs. (24)

$$I_o = -\frac{4}{\pi R^2}\int_0^R \bar{\varphi}_o(z_u)dy$$

where z_u is the value of z along the upper boundary of the slipstream. Making use of Eq. (18) with $y^2 + z^2 = R^2$, we obtain

$$I_o = \frac{1-\mu}{\pi\mu^{1/2}}\int_0^1 \left\{ \ln\left[\frac{1-az}{1+az} \right] \right\} (1-z^2)^{-1/2} z\, dz$$

where $a = 2\mu^{1/2}/(1+\mu)$. The integration may be evaluated (e.g., p. 86, No. 22a of Ref. 10), and we obtain

$$I_o = -(1-\mu) \tag{25}$$

Similarly, the integral I_s as defined in Eq. (24) may be written

$$I_s = \frac{1}{\pi R^2}\int_{S_{2s}} \frac{\partial \bar{\varphi}_s}{\partial z}\, dy\, dz = \frac{4}{\pi R^2}\int_0^R \bar{\varphi}_s(z_u)dy = -\frac{4}{\pi R^2}\int_0^R \bar{\varphi}_o(z_u)dy = I_o \tag{26}$$

where we recall $(\partial\bar{\varphi}_s/\partial z) = (\mu/w_\infty)(\partial\varphi_s/\partial z) - (1-\mu)$, and we have made use of Eq. (17) evaluated on the boundary.

The expression for G_o may be written

$$G_o = \frac{1}{\pi R^2}\iint_{S_{2o}} (\nabla \bar{\varphi}_o)^2 r dr d\theta$$

The gradient term may be evaluated from Eq. (18). However, it is more convenient to evaluate $\nabla\bar{\varphi}_o{}^2$ directly from the complex potential F_o. Thus, we obtain in polar coordinates

$$\nabla\bar{\varphi}_o{}^2 = \frac{(dF_o/dZ)(dF_o{}^*/dZ^*)}{w_\infty{}^2} = \frac{(1-\mu^2)R^4}{r^4 + R^4\mu^2 + 2r^2R^2\mu\cos 2\theta}$$

Substituting into the expression for G_o, we obtain

$$G_o = \frac{(1-\mu)^2}{\pi}\int_R^\infty r dr \int_0^{2\pi} \frac{R^2 d\theta}{r^4 + R^2\mu^2 + 2r^2R^2\mu\cos 2\theta}$$

The integral with respect to θ is $2\pi R^2/(r^4 - R^4\mu^2)$ (see Ref. 10). Thus, G_o becomes

$$G_o = 2(1-\mu)^2\int_R^\infty \frac{R^2 r dr}{r^4 - R^4\mu^2} = \frac{(1-\mu)^2}{2\mu}\ln\frac{1+\mu}{1-\mu} \tag{27}$$

Evaluation of G_s may be accomplished in a similar fashion through use of the complex potential for F_s [Eq. (15)] and with the definitions for $\partial\bar{\varphi}_s/\partial z$ and $\partial\bar{\varphi}_s/\partial y$. This gives

$$G_s = G_o \tag{28}$$

Evaluation of force coefficients

Substituting Eqs. (25–28) into Eq. (23) gives

$$X = \pi R^2\rho\left(u_s(u_s - u_o) + \left(\frac{1-\mu}{\mu^2}\right) w_\infty{}^2 \left\{ (1+\mu^2) \times \left[1 - \frac{1-\mu}{4\mu}\ln\left(\frac{1+\mu}{1-\mu}\right) \right] - \frac{1+\mu}{2} \right\} \right) \tag{29}$$

Carrying out a similar evaluation for the component of $\mathbf{T}$ in the z direction (the pressure forces do not contribute to this component) gives

$$Z = \pi R^2\rho(1-\mu)u_o w_\infty \tag{30}$$

It is convenient to express the forces on the actuator disk in terms of horizontal and vertical force coefficients C''_{H_p} and C''_{L_p}, based on the propeller area A_p and the dynamic pressure in the slipstream at ambient static pressure. Thus, we define

$$C''_{H_p} = (X\cos\delta - Z\sin\delta)/A_p(q_\infty + \Delta H)$$

$$C''_{L_p} = (X\sin\delta + Z\cos\delta)/A_p(q_\infty + \Delta H)$$

Substituting for Z and X through Eqs. (29) and (30), and using Eq. (11) for ΔH, we obtain, after some simplification

$$C''_{H_p} = \left(\frac{A_s}{A_p}\right) \times \frac{\{2(1-\mu) - (1-\mu)[1+\mu+g(\mu)]\sin^2\delta\}\cos\delta}{[(1-\mu^2)\cos^2\delta + \mu^2]} \tag{31}$$

$$C''_{L_p} = \left(\frac{A_s}{A_p}\right) \times \frac{\{2(1-\mu)(1+\mu^2) - (1-\mu)[1+\mu+g(\mu)]\sin^2\delta\}\sin\delta}{[(1-\mu^2)\cos^2\delta + \mu^2]} \quad (32)$$

where $g(\mu) = [(1+\mu^2)/(1-\mu)]G_o$ and $A_s = \pi R^2$ is the area of the fully contracted slipstream (vortex tube).

Since **T** is assumed to act normal to the plane of the disk, the tilt angle α_p is given by

$$\alpha_p = \tan^{-1}(C''_{L_p}/C''_{H_p}) \quad (33)$$

Introducing the thrust coefficient T''_c, defined as

$$T''_c = \frac{T/A_p}{q_\infty + \Delta H} = [(C''_{H_p})^2 + (C''_{L_p})^2]^{1/2} \quad (34)$$

the ratio of the propeller area to slipstream area A_p/A_s becomes

$$A_p/A_s = [(C''_{L_p}A_p/A_s)^2 + (C''_{H_p}A_s/A_p)^2]^{1/2}/T''_c \quad (35)$$

where the quantities $C''_{L_p}A_p/A_s$ and $C''_{H_p}A_p/A_s$ are given by Eqs. (31) and (32).

Equations (11 and 31–35) provide the relations needed to express the flowfield velocities in terms of the more convenient parameters T''_c, α_p, and A_p instead of μ, δ, and A_s. Once T''_c, α_p, aud A_p are known, μ, δ, and A_s may be obtained either by iterating on the value of δ, or graphically from Fig. 3.

Power

The power P added to the slipstream and to the outside flow by the actuator disk is readily obtained by evaluating the net flux of energy out of the cylindrical control surface in Fig. 2. Thus, writing

$$P = -\frac{\rho}{2}\int_{S_1+S_2+S_3}(\mathbf{V}\cdot\mathbf{V})(\mathbf{V}\cdot d\mathbf{S}) - \int_{S_1+S_2+S_3} p\mathbf{V}\cdot d\mathbf{S}$$

and performing a similar analysis to that done previously for the components of **T**, we obtain

$$P = u_s A_s \Delta H \quad (36)$$

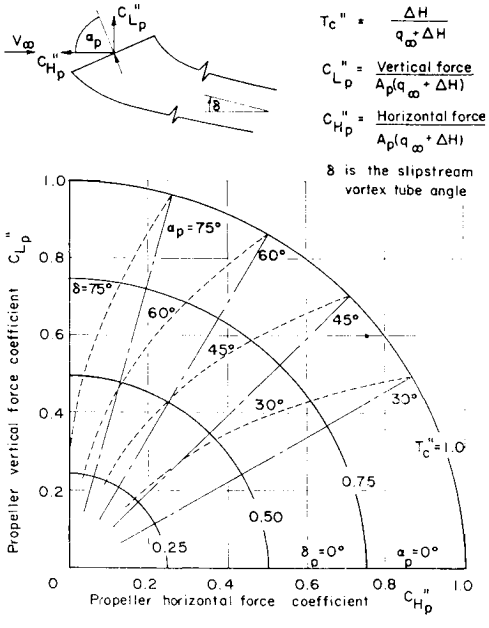

Fig. 3 Vortex tube angle, inclined actuator disk theory.

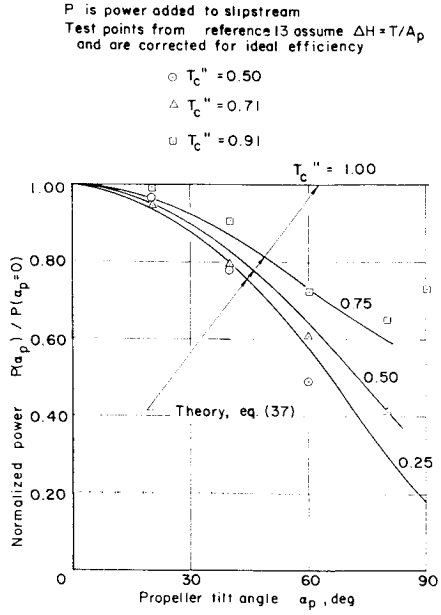

Fig. 4 Variation in power required with propeller tilt angle from inclined actuator disk theory.

The effect of propeller tilt angle on power, for a fixed forward velocity and thrust coefficient, is found by writing Eq. (36) as

$$\frac{P(\alpha_p)}{P(0)} = \left\{\frac{\cos^2\delta + [T''_c/(1-T''_c)]}{1 + [T''_c/(1-T''_c)]}\right\}^{1/2}\left[\frac{(A_s/A_p)(\alpha_p)}{(A_s/A_p)(0)}\right] \quad (37)$$

where δ and A_s/A_p are obtained in terms of α_p from Eqs. (11) and Eqs. (31–35). This expression has been evaluated (Fig. 4), and is compared with wind-tunnel measurements of power vs tilt angle in the following section.

Slipstream Rotation

In order to include effects of swirl in the present slipstream analysis, we assume an idealized vortex model of the propeller, viz., a bound vortex of constant strength Γ rotating with the blade. A line vortex is shed from the blade tip and moves rearward, because of the action of the freestream and because of self-induction effects, and forms a spiral-like trailing vortex system. A semi-infinite vortex of equal strength and lying along the slipstream axis must be inserted into the model to provide continuity with the bound vortex. The axial vortex induces swirl velocities inside the slipstream. In this model, the trailing vortices may be shown to have no effect on swirl inside the slipstream, but shield the axial vortex outside the slipstream, thereby reducing the resultant swirl velocities to zero.

Far enough behind the propeller, the trailing vortex spiral may be assumed infinite in extent. The axial velocity increment induced inside the slipstream [see also Eq. (3)] is then $u_s - u_o = \gamma = 2N\Gamma/(u_o + u_s)$ where the vortex strength per unit length γ is obtained by dividing Γ by the number of spiral loops per unit length. Here, N is the number of blade revolutions per unit time and $(u_o + u_s)/2$ is the average axial velocity of the trailing spiral. Since $\Delta H/\rho = \frac{1}{2}(u_s^2 - u_o^2)$, we obtain

$$\Gamma = JV_\infty R_p \Delta H/q_\infty \quad (38)$$

where J is the advance ratio.

Due to the axial vortex, the inviscid swirl velocity v_θ is found to be

$$v_\theta/V_\infty = (\Gamma/2\pi r V_\infty) = (J/2\pi)(R_p/r)(\Delta H/q_\infty) \quad (39)$$

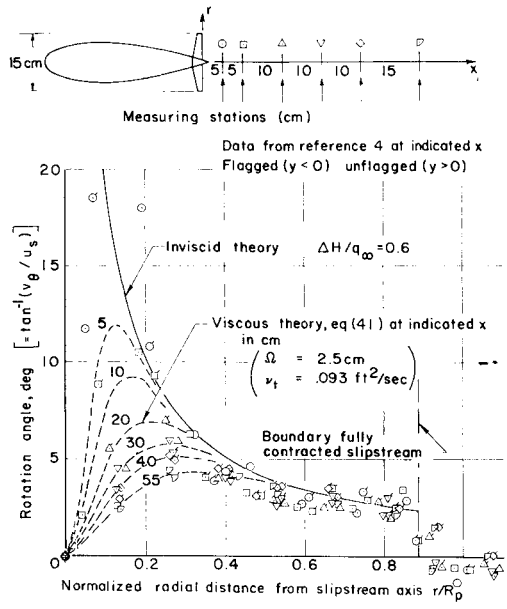

Fig. 5 Comparison with slipstream rotation angle test data from Ref. 4.

inside the slipstream, and

$$v_\theta/V_\infty = 0 \tag{40}$$

outside the slipstream.

This simple vortex model for slipstream swirl caused by the propeller rotation is similar to that of Franke and Weinig.[3] However, in order to keep the swirl velocities finite near the axis, the axial vortex will be "softened" by introducing viscous core effects according to Lamb.[11] The resulting expression for the circumferential swirl velocity $v_\theta(r)$ inside the slipstream is then

$$\frac{v_\theta}{V_\infty} = \pm \frac{J}{2\pi}\left(\frac{R_p}{r}\right)\left(\frac{\Delta H}{q_\infty}\right) \times \left\{1 - \exp\left[-\left(\frac{r}{R}\right)^2\left(\frac{R}{x+\Omega}\right)\left(\frac{Ru_s}{4\nu_t}\right)\right]\right\} \tag{41}$$

where $J = V_\infty/2NR_p$ is the advance ratio, ν_t is the effective turbulent viscosity, Ω is the effective starting distance ahead of the origin for the viscous core, and the sign is positive for a counter-clockwise sense of rotation when viewed from the rear.

Equation (41) is compared with measurements by Stüper[4] in Fig. 5. The test data were obtained at several stations in the wake of a 0.49-ft-diam pusher propeller aligned with the free stream and at a thrust coefficient $T''_c \simeq 0.38$. With the origin $x = 0$ located at the blade trailing edge, the best fit to the data was accomplished by choosing $\nu_t = 0.093$ ft²/sec and $\Omega = 0.08$ ft (approximately twice the maximum blade chord). The propeller advance ratio was 0.472, whereas the free-stream velocity was approximately 100 fps. The circulation Γ was 14.2 ft²/sec as computed from Eq. (38).

It is not clear how ν_t will scale for different values of these parameters, although, as discussed by Hall,[12] ν_t scaling with either Γ or $(\Gamma)^{1/2}$ has been considered. Because it would be premature to use such scaling laws indiscriminately, and because of the lack of additional test data on the slipstream vortex, the value $\nu_t = 0.10$ ft²/sec was used in all subsequent calculations and design charts.

Comparison with Propeller Test Data

Because of the many assumptions inherent in the inclined actuator disk theory, it is of importance that the theory be evaluated by comparing with test data before being applied to the wing-slipstream interference problem. Comparisons of the power and average downwash angle across the slipstream may be made without consideration of slipstream swirl. However, the swirl effects should be added to the theory before detailed downwash survey data may be compared.

A comparison between predicted and measured effects of propeller tilt angle on power is shown in Fig. 5. Both the theory, Eq. (37), and the test data, Ref. 13, show that the power required to produce a given value of T''_c decreases with increasing tilt angle, with the power becoming independent of tilt angle as $T''_c \to 1.0$, although considerable data scatter is present.

The downwash angle ϵ far behind the propeller may be found from the expression

$$\epsilon(y, z) = -\tan^{-1}[(w\cos\delta - u\sin\delta)/(w\sin\delta + u\cos\delta)] \tag{42}$$

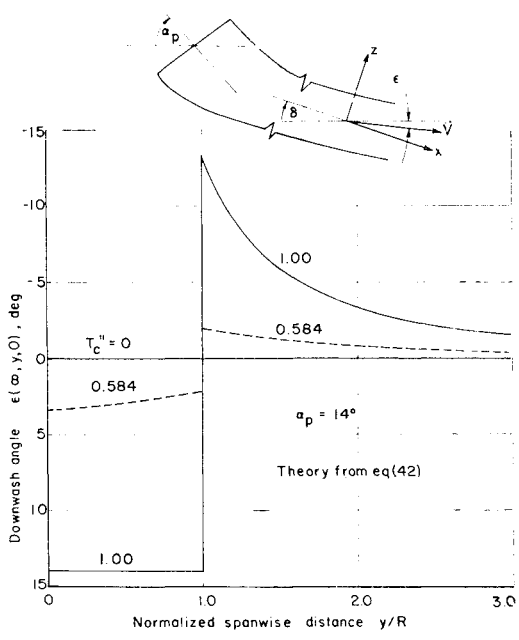

Fig. 6 Downwash angle across slipstream centerline, inclined actuator disk theory.

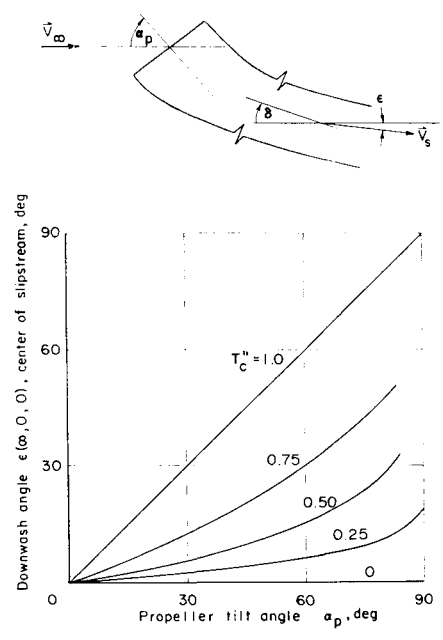

Fig. 7 Theoretical downwash angle on slipstream centerline, inclined actuator disk theory.

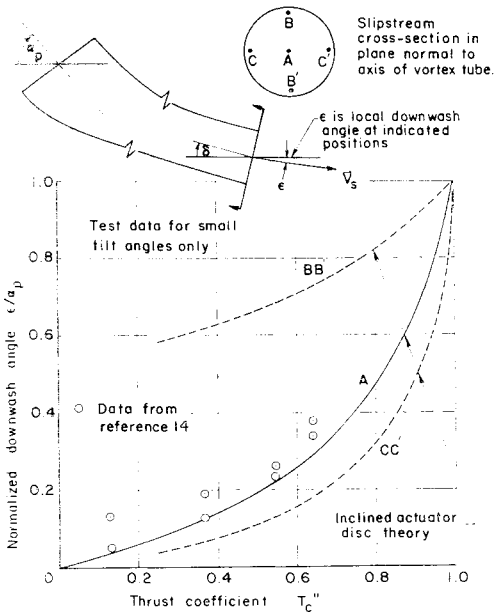

Fig. 8 Comparison with slipstream downwash angle test data.

and is readily determined from the theory using Eqs. (19) and (20). As illustrated in Fig. 6, Eq. (42) predicts a nonuniform downwash distribution inside the slipstream and a varying upwash outside the slipstream, except for the limiting cases $T''_c = 0$ and 1.0. The calculated downwash angle at the center of the slipstream has been plotted, for convenience, in Fig. 7.

The nonuniform value of ϵ makes comparison with test data, obtained by means of a tailplane spanning the slipstream, somewhat difficult to interpret. Nevertheless, as illustrated in Fig. 8, such "average" test data[14] show a variation in the ratio of ϵ/α_p with T''_c similar to that predicted by theory, at least for the small values of α_p for which the tests were conducted.

References

[1] Koning, C., "Influence of the Propeller on Other Parts of the Aircraft Structure," *Aerodynamic Theory*, edited by W. F. Durand, Vol. IV, Div. M, Dover, New York, 1935, pp. 361–431.

[2] Glauert, H., "The Lift and Drag of a Wing Spanning a Free Jet," R and M 1603, 1934, British Aeronautical Research Council.

[3] Franke, A. and Weinig, F., "The Effect of the Slipstream on an Airplane Wing," TM 920, 1939, NACA.

[4] Stüper, J., "The Effect of Propeller Slipstream on Wing and Tail," TM 874, 1938, NACA.

[5] Graham, E. W. et al., "A Preliminary Theoretical Investigation of the Effects of Propeller Slipstream on Wing Lift," Rept. SM-14991, 1953, Douglas Aircraft Co.

[6] Ribner, H. S., "Theory of Wings in Slipstream," Rept. 60, 1959, Institute of Aerophysics, Univ. of Toronto.

[7] Ellis, N. D., "A Computer Study of a Wing in a Slipstream," TN 101, 1967, Institute for Aerospace Studies, Univ. of Toronto.

[8] Ribner, H. S. and Ellis, N. D., "Theory and Computer Study of a Wing in a Slipstream," AIAA Paper 66-466, Los Angeles, Calif., 1966.

[9] Brenckmann, M., "Experimental Investigation of the Aerodynamics of a Wing in a Slipstream," *Journal of Aeronautical Sciences*, Vol. 25, No. 5, May 1958, pp. 324–328.

[10] Grobner, W. and Hofreiter, N., *Integral Tafel, Zweiter Teil, Bestimmte Integrale*, Springer-Velag, Vienna, Austria, 1961.

[11] Lamb, H., *Hydrodynamics*, Cambridge University Press, 1932.

[12] Hall, M. G., "The Structure of Concentrated Vortex Cores," *Progress in Aeronautical Sciences*, Vol. 7, edited by D. Kuchemann, Pergamon, London, 1966.

[13] Kuhn, R. E. and Draper, J. W., "Investigation of the Aerodynamic Characteristics of a Model Wing-Propeller Combination and of the Wing and Propeller Separately at Angles of Attack up to 90°," TR 1263, 1956, NACA.

[14] Simmons, L. F. G. and Ower, E., "Investigation of Downwash in the Slipstream," R and M 882, 1923, British Aeronautical Research Council.

[15] Levinsky, E. S. et al., "Lifting Surface Theory and Tail Downwash Calculations for V/STOL Aircraft in Transition and Cruise," TR 68-67, Oct. 1968, U.S. Army Aviation Labs.